Accuracy Improvement of Nano-fiber Deposition by Near-Field Electrospinning

Jiachen Xu[1,#], Maxwell Abecassis[1], Zixuan Zhang[1], Ping Guo[1], Jiaxing Huang[2], Kornel Ehmann[1] and Jian Cao[1]

1 Department of Mechanical Engineering, Northwestern University, IL, USA
2 Department of Materials Science and Engineering, Northwestern University, IL, USA
Corresponding Author / E-mail: jiachenxu2013@u.northwestern.edu, TEL: +84-7-563-0083

KEYWORDS : Near-Field Electrospinning, Nanofiber, Electrohydrodynamics

Developed from the far field electrospinning (FFES) process, near-field electrospinning (NFES) holds the promise to become a direct-writing technology with high throughput and multi-material capability not only in 2D but also in 3D space. The underlying problem is the deposition of fibers on top of each other. Since the fibers are of sub-micron size, the accuracy of the deposition must reach the same level to realize this requirement. Deposition inaccuracy is attributable to numerous sources including the residual charges remaining on the deposited fibers that repel the fiber being deposited as well as the inappropriate shape of the electric field guiding the deposition process. To eliminate these two influences, this paper proposes two possible solutions. In the first, the polarity of the electrodes is being switched in subsequent deposition passes, while in the second the ground electrode plate is replaced by a grounded pin to modify the shape of the electric field. A comparative experimental analysis of the feasibility of these two methods is presented and their advantages and disadvantages are discussed.

1. Introduction

Electrohydrodynamic (EHD) principles have long been applied in the manufacture of sub-micron structures. One example is the far field electrospinning (FFES) process dating back to the 1930s[1-3] for making fine textile fibers. In this process a high voltage (in the kV range) is applied between a spinneret and a collector for pulling continuous polymer fibers from a solution or melt. FFES can generate nanoscale polymer fibers but lacks the control over registry or alignment due to: (1) bending instability, (2) splitting of the fibers during elongation due to electrostatic repulsion between charged segments, and (3) fiber buckling upon landing on the collector due to electrostatic repulsion between the already deposited segments and incoming segments[4, 5] (**Fig. 1**). At the beginning stage when the bending perturbations are negligible, the liquid jet is straight.[6] This portion of the jet has been recently utilized to deposit highly aligned fibers in the so-called near-field electrospinning (NFES) process.[7]

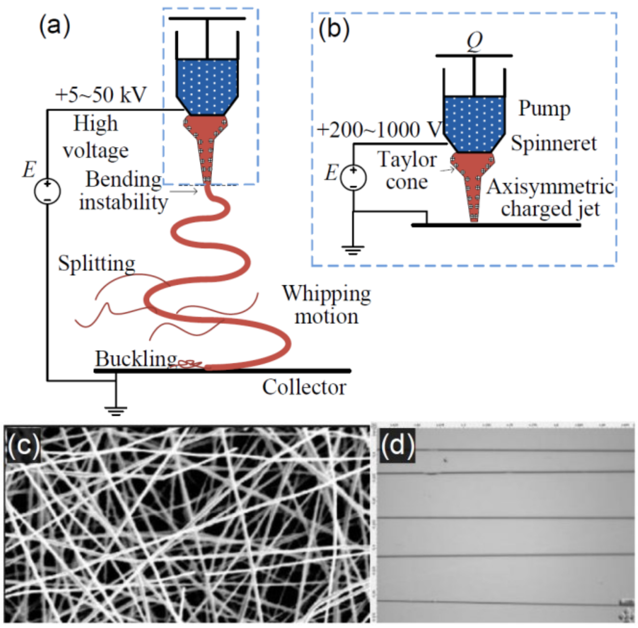

Fig. 1 Schematic illustration of (a) far-field electrospinning and (b) near-field electrowriting processes, which produce (c) random[8] and (d) aligned nanofibers, respectively.

In the current research, NFES is being proposed to deposit fibers not only in 2D but in 3D space. In other words, the underlying problem is the deposition of fibers on top of each other.

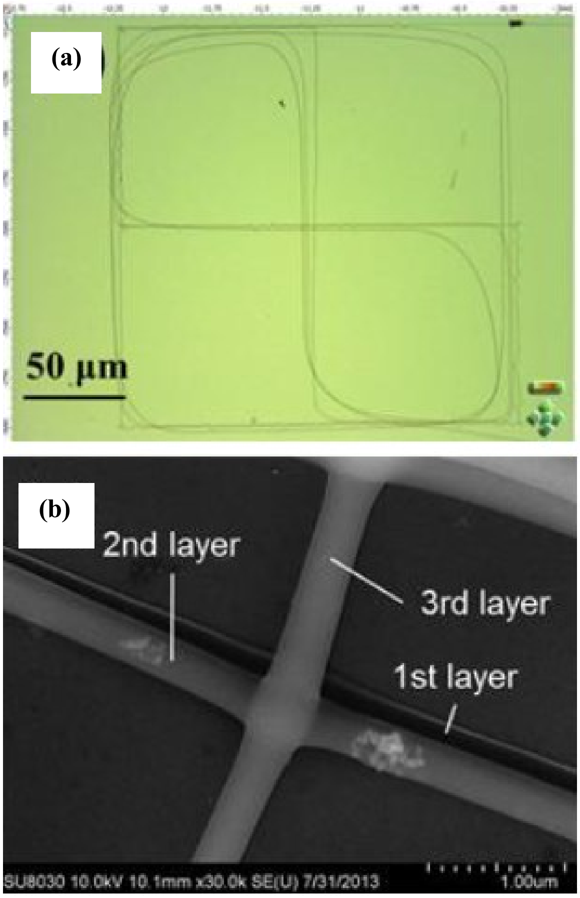

Fig. 2 Deposited multilayer patterns of sub-micron PEO fibers shown by (a) Optical microscopy and (b) SEM images

Deviations in the accuracy of deposition can be clearly identified from **Fig. 1d** and **Fig. 2a**. There are mainly two deposition errors that need to be minimized. The first one is the alignment of straight lines. As it can be seen in **Fig. 1d**, a constant gap between adjacent lines of deposited nanofibers is not maintained. The second, shown in **Fig. 2b**, is related to the sharpness of the corners of the nanofiber square. In this paper, two novel methods that contribute to the enhancement of deposition accuracy to alleviate these problems will be described.

2. Experimental Setup and Procedures

2.1 Experimental Setup

The preliminary setup for electrospinning tests is shown in **Fig. 3**. A high molecular weight polyethylene oxide (PEO, MW=4,000,000) solution was prepared at 2 wt% and loaded into a glass syringe. The needle used is of gauge 30, with an inner diameter of 0.15 mm. The pump is a screw-drive type actuator driven by a stepping motor. An enclosure is built to isolate the deposition from outside airflows and environmental influences. The collector, or the ground electrode, is mounted to a precision wedge motion stage. The motion is composed of two side wedges and a center wedge. The two side wedges move in the X-axis direction; their relative motion determines the Z-axis motion. When the two side wedges move towards each other, the center wedge raises; while when they move apart from each other, the center wedge drops. An independent Y-axis slide is installed on the top of the center wedge. With this wedge design, the stiffness of the machine and the resolution of the Z-axis are increased. The resolution in the X- and Y-axes is 50 nm; the resolution in the Z-axis is increased by a factor inversely proportional to the tangent of the wedge angle. The stage is controlled by a Delta-Tau UMAC system. A Labview program provides the user interface for the controller. The deposition process is monitored by a microscopic camera. The voltage kept between the needle and the ground ranged between 300-1500 V. The needle-to-collector distance (Z-axis) was set between 1-3 mm.

2.2 Experimental Procedures

Two types of experiments were performed and will mainly be discussed in this paper. They are performed by using a Zig-Zag or a Back-Forth motion trajectory. The

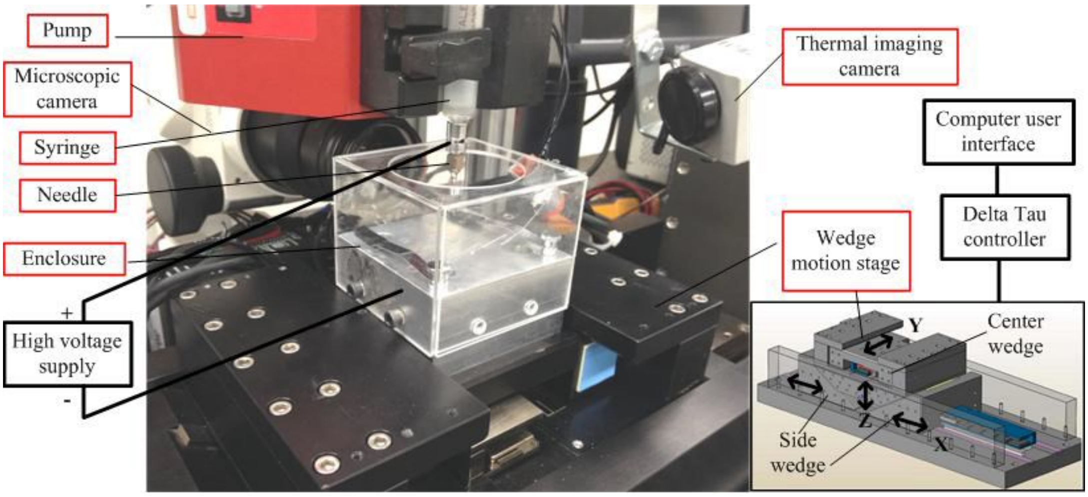

Fig. 3 Preliminary version of the NFEW system setup

schematic of the Zig-Zag motion is shown in **Fig. 4** that becomes a Back-Forth motion when Delta Y is equal to 0, during which the stage basically moves back and forth along the same straight line trajectory. The advantage of applying these motion trajectories is that the deposition accuracy problem can be characterized by simple parameters. In this paper, only the Back-Forth motion trajectory will be used to test repeatability and accuracy, because the deviations under this circumstance are more obvious under the microscope. In the set of experiments below, Delta X was set as 8,000 μm and Delta Y as 0. The feed along the X-axis was 1,000 μm per second.

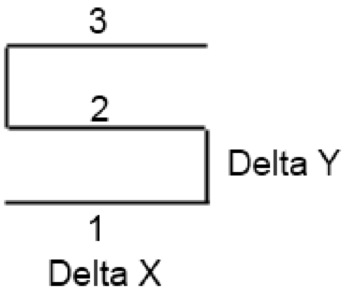

Fig. 4 Schematic of the Zig-Zag and Back-Forth (Delta Y = 0) motions

It should be mentioned that before each tests, the surface tension at the tip of the needle was broken manually by a stick to trigger the deposition process. In other words, the very first fiber has to be pulled out onto the collector manually. Otherwise, the electric field applied between the needle and the ground plate would only distort the shape of the bubble instead of starting the pulling and deposition of the nanofiber.

2.3 Calibration and Compensation of Stage Inaccuracies

Although with the wedge design used, the stiffness of the machine and the resolution of the Z-axis were considerably increased, deposition accuracy problems attributable to numerous sources remain. One of the possible components is due to deviations of the stage motions from the theoretical trajectory.

Before any experiments were conducted, the inaccuracy from the stage were quantified and compared to the deposition process itself to make sure it is negligible.

The running deviation of the stage can be alleviated through high resolution measurement equipment and metrology. In the stage used, the X-axis is coupled with the Z-axis, which means that the X- and Z-positions depend on the combination of two motors and have to be considered simultaneously. The Y-axis is, in turn, is independent and thus can be compensated independently.

In this case, a laser calibration system HP5529A with a resolution of 10 nm was used to calibrate the three-axis translation stage. The position in the X-, Y-, and Z-directions were measured using system and the errors are calculated accordingly to obtain compensation tables used in the control system of the stage. Finally, the linear positioning is measured again to examine the performance of the stage after compensation.

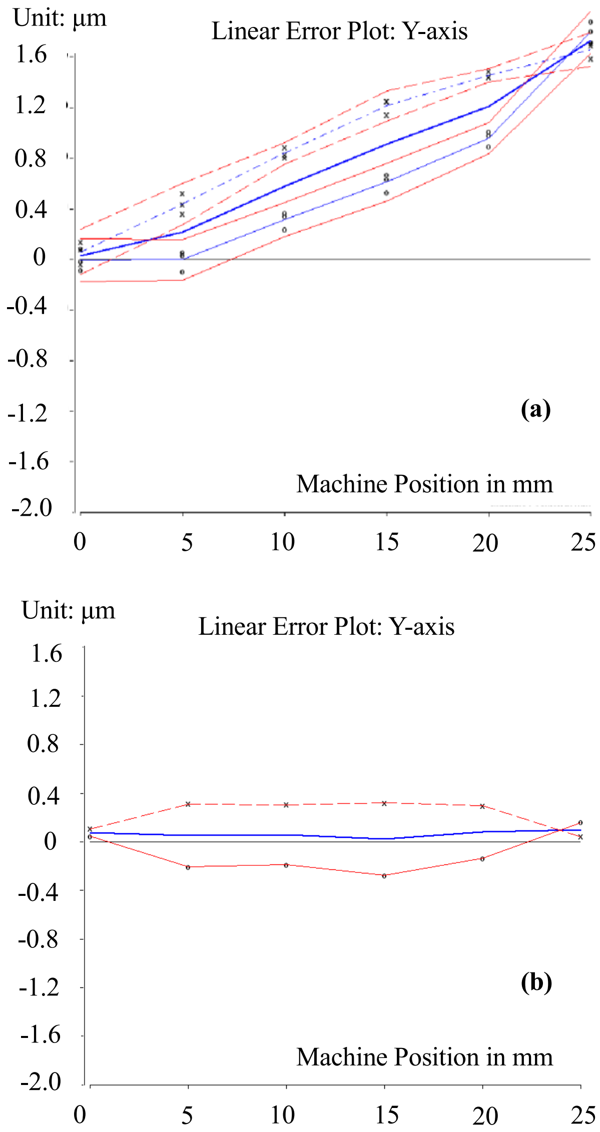

Fig. 5 Calibration result of the Y-axis: (a) before calibration (b) after calibration

Above is an example of the result from the Y-axis calibration. The deviation range was reduced and balanced from -400 nm to +2,000 nm to -400 nm to +400 nm. The examination of the deviations shown in **Fig. 6,** leads to the conclusion that the deviation of the stage is rather negligible in comparison to the deviations originating from the deposition process itself.

2.4 Experimental Result from the Customary Normal Procedure

The results from a normal Back-Forth deposition process with a 1,250 Voltage between the needle and the ground after compensation are shown in **Fig. 6**.

Given that the experiments shown in **Fig. 6** utilized the Back-Forth motion trajectory, the nanofibers are supposed to be straight and deposited theoretically along the same line. In other words, during the deposition process the fiber in the air should follow a straight line trajectory perpendicular to the ground electrode. However, in reality this is not the case as evidenced by **Fig. 6. T**hree major problems can be observed: (1) the fibers are too far apart from each other, (2) the fibers are not parallel to each other, and (3) each deposited nanofiber line has several twisted areas along the line and thus not straight enough. As it can be seen, the average gap between the deposited fibers is around 74 µm instead of the expected 0 µm given that they were deposited along the same linear trajectory.

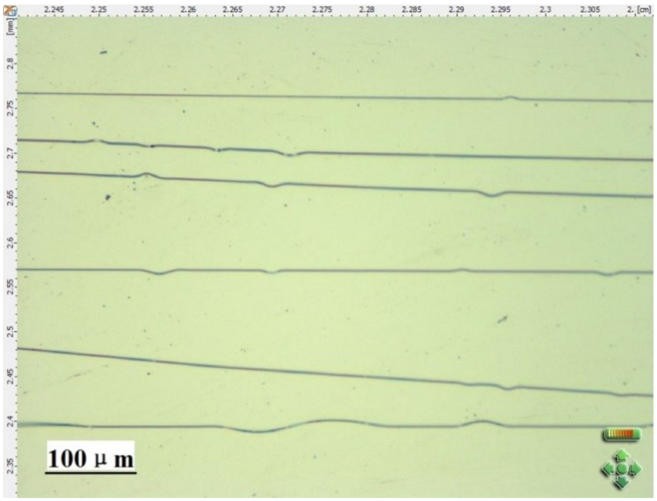

Fig. 6 Optical microscopy of a normal Back-Forth deposition

The deviations observed in **Fig. 6**, are attributable to a number of sources including: (1) the bending instability, shown in **Fig 1a**, although more pronounced in the FFES, also effects the NFES process by preventing the fiber that is being pulled out of the solution bubble from maintaining a vertical straight line; (2) the insufficient strength of the electric field to guide the fiber or the it has a centrifugal component that deflects the fiber in the air away from being attached to the area vertically under the needle on the collector; and (30 the residual charges resulting in the repulsion of the fiber being deposited, which also influence the deposition accuracy. These phenomena will be further illustrated in the following sections.

In order to alleviate or overcome the above-described problems experimentally demonstrated under normally applicable circumstances in the subsequent Sections two novel procedures aimed at enhancing deposition accuracy will be presented. In the first procedure, under the assumption that residual charges are the dominant factor influencing accuracy, a method that switches system polarity in subsequent passes will be explored. In the second, an additional electrode is being introduced to change the shape of the electric field.

3. Eliminating the Influence of Residual Charges

3.1 Concept and Setup

The electrostatic repulsion between the deposited structures and the structures being deposited, shown in **Fig. 7,** is a potential phenomenon contributing to deposition inaccuracy. One possible solution to overcome this influence that is explored here is to flip the polarity of the electrodes in successive deposition passes. In other words, the residual charges on the fiber being deposited would be the opposite of the charges on the deposited fibers and thus attractive to each other. Such a procedure would possibly result in an additional benefit of enhancing the stability of deposition.

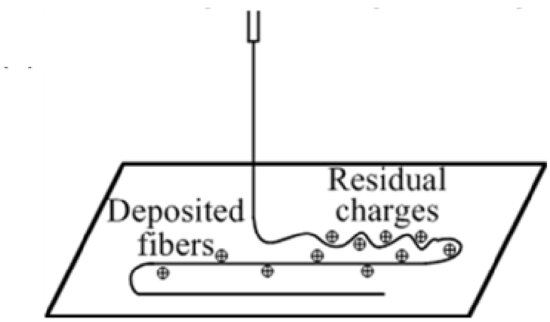

Fig. 7 Deposited fibers repel landing fibers due to dissipated residual charges

The experimental setup is similar to the setup used for the customary process. A Back-Forth experiment is used to test the possible consequences from the above-proposed procedure. In the experiments performed, the polarity of the poles of the electrode at the end of each segment/pass was manually switched. In both tests the syringe was heated to 48 ˚C to prevent the fibers from drying.

3.2 Experimental Results

The tests were carried out under the same voltage levels as the tests in the normal case. As expected, the procedure resulted in better aligned deposited fibers as depicted in **Fig. 8**. Compared to the results performed under normal conditions (**Fig. 6**), the fibers are more concentrated. The average gap decreased from 74 µm to about 20 µm and the fibers are more parallel to each other. This improvement can hence dramatically benefit the deposition accuracy.

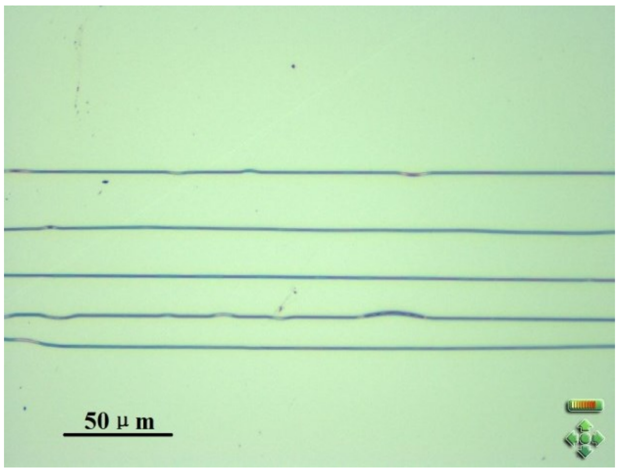

Fig. 8 Optical microscopy in the middle of a Back-Forth deposition with flipping poles

A potential disadvantage of the process can be noticed in **Fig. 9** depicting the end of a segment. The disorder at the end of each segment is essentially caused by the flipping of the polarity. It was observed by the microscopic camera during the experiments, that immediately after the polarity is being flipped, the electric field also changes direction. As a consequence this causes the deposited fiber of being pulled up into the air and leads to the observed disruption at the end of the segments. Concurrently, the electric charges in the bubble under the needle also change polarity. Since the fiber between the needle and the collector is still connected to the bubble, the surface tension of the solution bubble under the needle does not need to be again manually broken and the subsequent fiber can easily overcome the surface tension and continue to deposit. This results in the continuance of pulling the fiber out from the bubble. Essentially, the phenomenon occurring while flipping the polarity is that the bottom half of the fiber being deposited and some of the fibers that are already deposited are attracted to the syringe while the top of the fiber being deposited continues to be pulled out from the bubble and deposited on the collector.

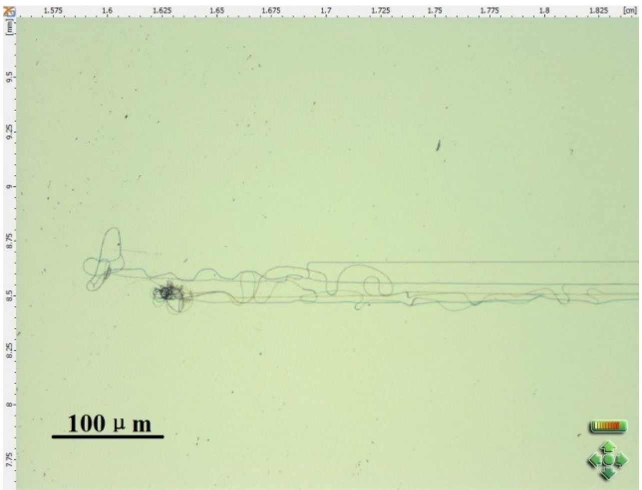

Fig. 9 Optical microscopy at the end of a Back-Forth deposition with flipping poles

It has also been observed that under certain conditions when the electric field is large enough or the fiber in the air dries out quickly enough, the fiber being deposited snaps after flipping. However, this type of snapping phenomenon is quite different from that occurring in the normal experiments. When snapping occurs in a normal experiment, it mostly happens at the connection point between the fiber and the bubble, in which case the surface tension of the solution bubble restores and the deposition process does not continue until the surface tension is manually broken again.

4. Changing the Shape of the Electric Field Lines

4.1 Concept and Setup

As it is shown in **Fig. 10a**, the normal customary setup uses a plate as the negative electrode which generates an equipotential surface that disperses the electric field lines and decreases the electric field density at the deposition point right under the needle on the collector. In addition, if the fiber between the needle and the collector is not vertically straight, which means it is off-centered from the point directly below the needle on the collector, the electric field will have a centrifugal component E_x that will further deflect the fiber leading to a stability problem. To overcome this problem the setup shown in **Fig. 10b** is being proposed. It not only increases the electric field density, but the electric field right above the collector will also have a centripetal component E_x which will stabilize the deposition process and increase its accuracy.

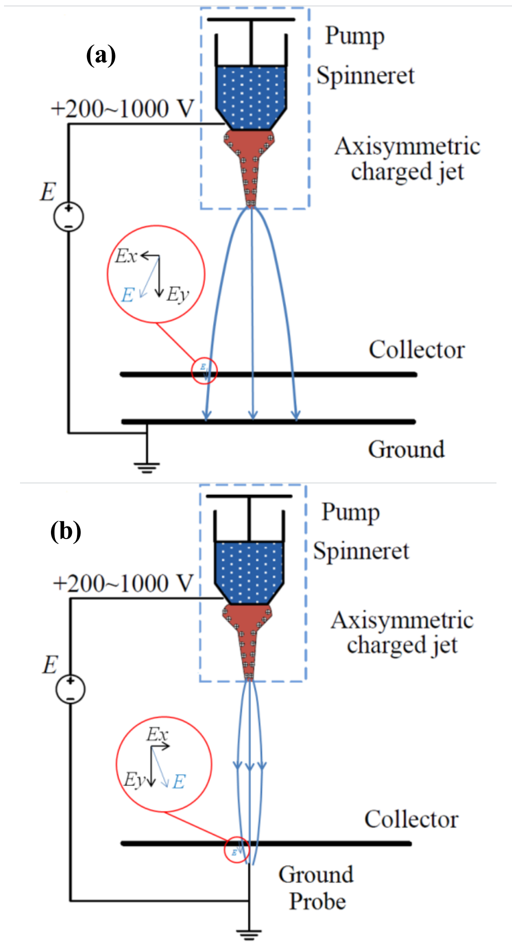

Fig. 10 Shape of electric field lines for (a) Current/Normal set up and (b) Proposed set up

The electrospinning test-bed used in the previous experiments, was revised according to the schematics shown in **Fig. 10b** and is depicted in **Fig. 11.** The aluminum block originally used for the ground electrode was replaced by an uninsulated copper wire which was kept stationary with respect to the needle during the process. The wire was carefully adjusted and aligned with the needle. Subsequently, a silicon collector was placed in the middle between the needle and the wire, as shown in **Fig. 11b,** and mounted on the enclosure which was, in turn, bolted to the wedge motion stage as shown in **Fig. 3**.

The bottom electrode is placed as close as possible to the silicon collector. The distance between the top needle and the collector and the voltage between the two electrodes were maintained at the same values as in the previous tests.

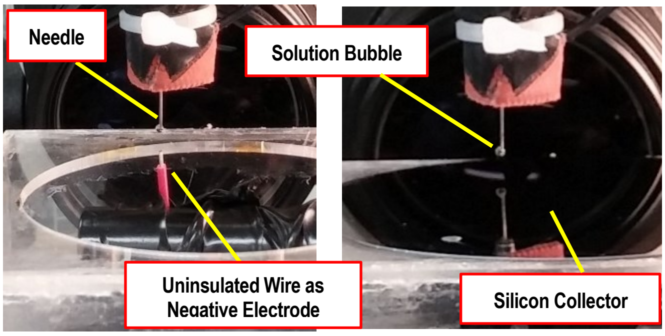

(a) (b)

Fig. 11 Revised setup (a) without collector and (b) with collector

4.2 Experimental Results

A Back-Forth test was again performed at 1,250V which is the same as in the normal tests in **Fig. 6**. The result is shown in **Fig. 12** from which it can be seen that the average gap decreases to as small as 7 μm, about 1/10 of the gap obtained under normal conditions. In particular, the four lines in the center almost pile up onto each other and at some point even merge together. This result clearly points to the feasibility, and clearly requiring further investigations, to expand the application of NFES from 2D to 3D printing.

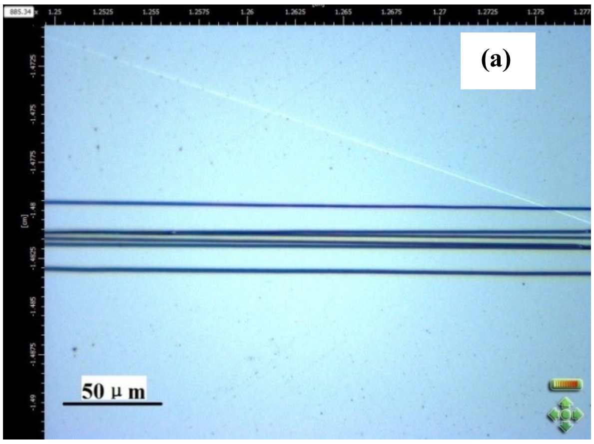

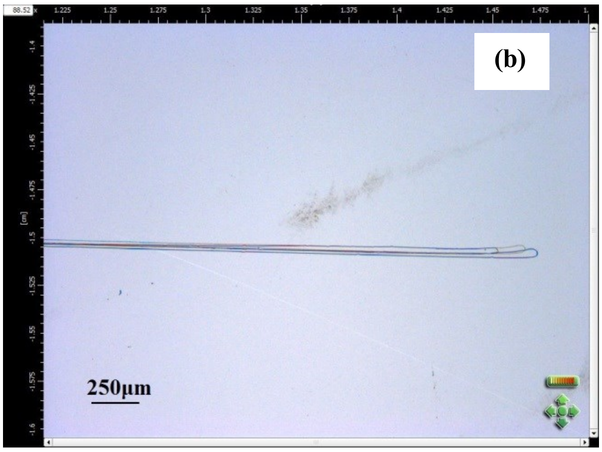

Fig. 12 Optical microscopy (a) in the middle (b) at the end of a Back-Forth deposition with dual-needle electrodes

5. Conclusions and Future Work

Near-field electrospinning (NFES) is a cutting edge process that has the potential to become a direct-writing technology with high throughput and multi-material capability. In order to generate more complex and accurate geometries and even achieve the goal of depositing in 3D space in the future, the deposition accuracy must approach sub-micron levels. For this purpose, two methods to further improve the deposition accuracy have been proposed. The Back-Forth experiment was adopted to test deposition accuracy using two different methods. The average gap between fibers was used to quantify the deviation of the results. Table 1 shows the comparison of different methods.

Table 1 Comparison of different methods

Method	Average Gap
Normal	74 μm
Flipping Polarity	20 μm
Dual-Needle Electrodes	7 μm

It can be concluded that both proposed methods indeed improve the accuracy of the deposition. However, the fact that the method based on flipping the polarity (Section 3) causes chaos at the flipping point suggests that it is most likely not a good procedure for continuous deposition. The method based on changing the electric field (Section 4), on the other hand, not only dramatically decreases the instability during the process, but is also very easy to adopt.

Several works remain to be performed in the future in order to further enhance the NFES process towards the sub-micron scale technology for direct writing of nanofibers into 3D patterns. The first is to illustrate the theoretical mechanism governing the fiber deposition process. For this purpose, analytical methods should be adopted to analyze the different physical mechanisms that are taking place. Second, to meet the demand of using a wide range of materials, different materials should be considered in NFES to study the relationship between the material characteristics and the process parameters. Finally, more accurate and sensitive instruments including gated cameras should be used to capture the details during the deposition process and compare them to the theoretical conclusions.

ACKNOWLEDGEMENTS

The support of the National Science Foundation (NSF) under grant CMMI-1404489 is gratefully acknowledged. This work has made use of the Optical Microscopy and Metallography (OMM) Facility supported by the MRSEC Program of the National Science Foundation (DMR 1121262).

REFERENCES

1. Anton, Formhals. "Process and apparatus for preparing artificial threads." U.S. Patent No. 1,975,504. 2 Oct. 1934.
2. Anton, Formhals. "Method and apparatus for spinning." U.S.

Patent No. 2,349,950. 30 May 1944.

3. Norton, Charles L. "Method of and apparatus for producing fibrous or filamentary material." U.S. Patent No. 2,048,651. 21 Jul. 1936.
4. Reneker, D. H., et al. "Electrospinning of nanofibers from polymer solutions and melts." Advances in applied mechanics 41 (2007): 43-346.
5. Reneker, Darrell H., et al. "Bending instability of electrically charged liquid jets of polymer solutions in electrospinning." Journal of Applied physics 87.9 (2000): 4531-4547.
6. Huang, Zheng-Ming, et al. "A review on polymer nanofibers by electrospinning and their applications in nanocomposites." Composites science and technology 63.15 (2003): 2223-2253.
7. Sun, Daoheng, et al. "Near-field electrospinning." Nano letters 6.4 (2006): 839-842.
8. Dzenis, Y. "Material science. Spinning continuous fibers for nanotechnology." Science (New York, NY) 304.5679 (2004): 1917-1919.
9. K. Salaita et al., "Massively Parallel Dip–Pen Nanolithography with 55 000 - Pen Two - Dimensional Arrays," Angew. Chem., 2006; 118: 7378-7381.
10. I. Gibson et al., Additive manufacturing technologies: rapid prototyping to direct digital manufacturing, Editor, Springer: 2010.
11. K. Hon et al., "Direct writing technology—advances and developments," CIRP Annals-Manufacturing Technology, 2008; 57: 601-620.
12. B. Li et al., "Robust direct-write dispensing tool and solutions for micro/meso-scale manufacturing and packaging," Proceedings of the ASME International Manufacturing Science and Engineering Conference: 2007.
13. G. Vozzi et al., "Microsyringe-based deposition of two-dimensional and three-dimensional polymer scaffolds with a well-defined geometry for application to tissue engineering," Tissue engineering, 2002; 8: 1089-1098.
14. J.-U. Park et al., "High-resolution electrohydrodynamic jet printing," Nature Mater., 2007; 6: 782-789.
15. S. Agarwal et al., "Use of electrospinning technique for biomedical applications," Polymer, 2008; 49: 5603-5621.
16. S.G. Kumbar et al., "Recent patents on electrospun biomedical nanostructures: an overview," Recent Patents on Biomedical Engineering, 2008; 1: 68-78.
17. C. Chang et al., "Direct-write piezoelectric polymeric nanogenerator with high energy conversion efficiency," Nano Lett., 2010; 10: 726-731.
18. Z. Liu et al., "Piezoelectric properties of PVDF/MWCNT nanofiber using near-field electrospinning," Sens. Actuators, A, 2013; 193: 13-24.
19. Z. Dong et al., "Electrospinning materials for energy-related applications and devices," J. Power Sources, 2011; 196: 4886-4904.
20. Z. Zhou et al., "Graphene-beaded carbon nanofibers for use in supercapacitor electrodes: Synthesis and electrochemical characterization," J. Power Sources, 2013; 222: 410-416.
21. A. Gomez et al., "Charge and fission of droplets in electrostatic sprays," Physics of Fluids, 1994; 6: 404.
22. A. Yarin et al., "Bending instability in electrospinning of nanofibers," J. Appl. Phys., 2001; 89: 3018.
23. D.W. Hutmacher et al., "Melt electrospinning," Chemistry–An Asian Journal, 2011; 6: 44-56.
24. G. Zheng et al., "Precision deposition of a nanofibre by near-field electrospinning," J. Phys. D: Appl. Phys., 2010; 43: 415501.
25. C. Chang et al., "Continuous near-field electrospinning for large area deposition of orderly nanofiber patterns," Appl. Phys. Lett., 2008; 93: 123111-123111-123113.
26. G.S. Bisht et al., "Controlled continuous patterning of polymeric nanofibers on three-dimensional substrates using low-voltage near-field electrospinning," Nano Lett., 2011; 11: 1831-1837.
27. W. Teo et al., "A review on electrospinning design and nanofibre assemblies," Nanotechnology, 2006; 17: R89.
28. J.A. Matthews et al., "Electrospinning of Collagen Nanofibers," Biomacromolecules, 2002; 3: 232-238.
29. S.Y. Chew et al., "Sustained release of proteins from electrospun biodegradable fibers," Biomacromolecules, 2005; 6: 2017-2024.
30. J.M. Deitzel et al., "Controlled deposition of electrospun poly(ethylene oxide) fibers," Polymer, 2001; 42: 8163-8170.
31. D. Li et al., "Electrospinning of Polymeric and Ceramic Nanofibers as Uniaxially Aligned Arrays," Nano Lett., 2003; 3: 1167-1171.
32. J. Lee et al., "Fabrication of patterned nanofibrous mats using direct-write electrospinning," Langmuir, 2012; 28: 7267-7275.